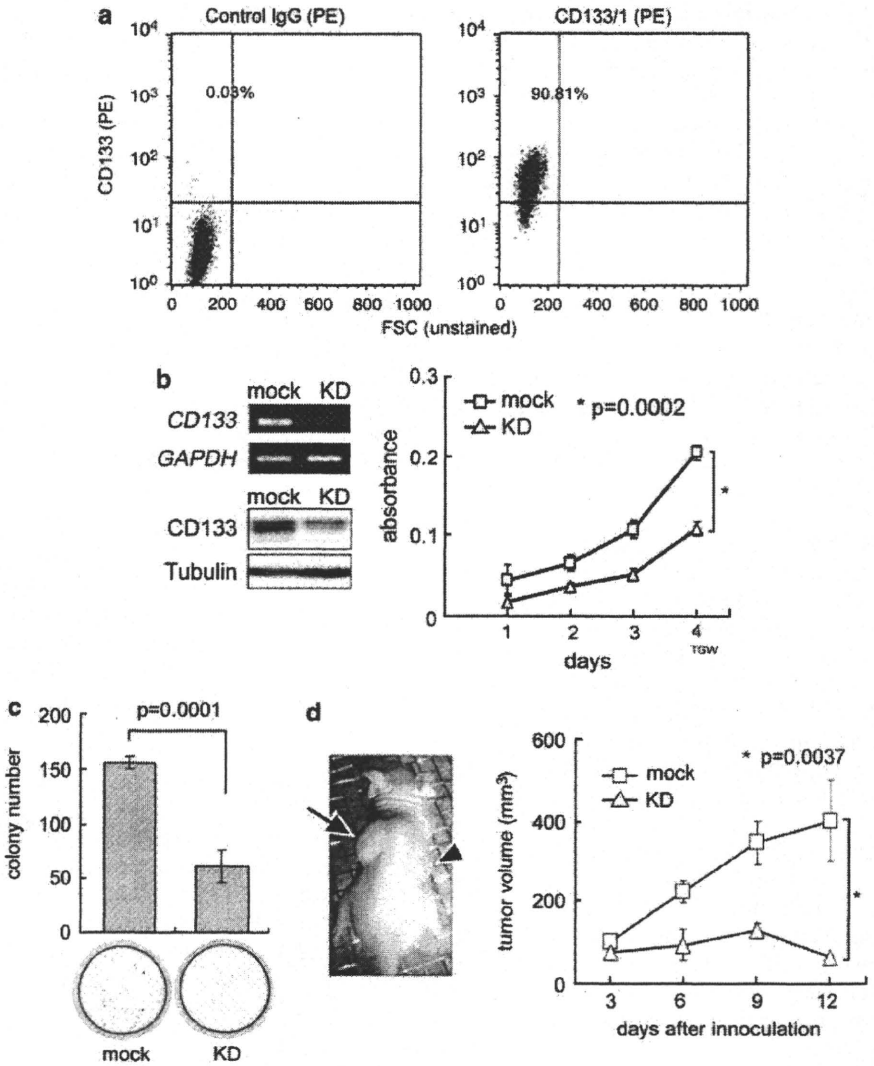

Figure 1 *CD133* knockdown inhibits the growth of human neuroblastoma (NB) cells. (**a**) Flow cytometric analysis of CD133 expression profiles in TGW cells. CD133 fluorescence is depicted on the *y* axis, and the percentage of CD133-positive cells is shown in the left upper corner of each plot. (**b**) Stable knockdown of *CD133* by lentivirus-mediated shRNA was performed as described in Materials and methods. *CD133* expression was detected by semi-quantitative RT–PCR and western blotting analysis in TGW cells. Growth curves were obtained by WST-8 assay. Anchorage-independent colony formation (**c**) and *in vivo* tumorigenic assay (**d**). TGW cells were stably transduced with shRNA against mock or CD133 (KD). (**c**) Colonies were stained with MTT dye and directly counted under a phase contrast microscope. (**d**) Tumor development in BALB/c AJcl *nu/nu* mice on injection of TGW cells stably infected with shRNA against mock (arrow) and CD133 (KD, arrowhead) cells. Tumor volume was measured every 3 days. Data are presented as the mean ± s.d. of tumors in four mice.

the effects of CD133 on *TrkA/B/C*, *p75NGFR* and *GDNF* expressions did not show a specific tendency. CD133 knockdown clearly increased *RET* mRNA (*RET* induction was 2.5–3.0-fold by qPCR). CD133-mediated RET downregulation was also observed at the protein level (Figure 3b). Furthermore, CD133 expression in primary NB spheres resulted in transcriptional suppression of *RET* (Figure 3c). These results suggest that CD133 suppresses *RET* gene transcription in NB cells.

To study the expression pattern of *CD133* and *RET* mRNA in human NBs, we performed semi-quantitative RT–PCR. *CD133* was expressed in 7 of 20 NB cell lines tested (Figure 3d), and only 1 NB cell line was *RET* positive in the 7 cell lines. We further studied *CD133* and *RET* expression in unfavorable patient-derived tumors (stages 3 and 4, TrkA(−), *MYCN* amplified). Again, *RET* expression was profoundly repressed in CD133-expressing NB tumors (Figure 3e). Finally, we studied the transcriptional activity of *RET* promoter in CD133-expressing cells. *RET* promoter reporter-derived luciferase activity was significantly suppressed in CD133-expressing cells (Figure 3e).

CD133 regulates NB cell differentiation in a RET-dependent manner

We investigated the biological effects of CD133 overexpression on *RET* downregulation in SH-SY5Y cells.

Significant neurite outgrowth was observed when mock-infected cells were stimulated with GDNF (Figure 4a). At the same time, no obvious difference was observed between mock- and GDNF-treated CD133-expressing cells. These results implied that CD133 overexpression inhibited NB cell differentiation.

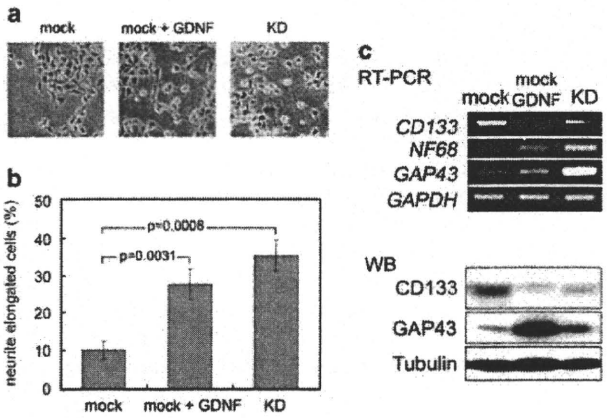

Figure 2 CD133 silencing induces differentiation in TGW cells. TGW cells were infected with lentivirus vectors encoding shRNA against *CD133* (right) or a mock (left) as a negative control. Ten days after infection, cells were treated with buffer (mock and KD) or GDNF (10 ng/ml, middle). Cells were scored for the presence of neurites longer than one cell diameter 72 h after treatment (photo: (**a**), bar graphs: (**b**)). Data are presented as the mean ± s.d. from at least three independent experiments. Statistical analysis was performed by Student's *t*-test. (**c**) NB differentiation-related molecule *neurofilament 68 (NF68)* and *GAP43* expressions in RT–PCR and WB. NF68 protein was not detected by WB in TGW cells.

We examined the effect of the co-expression of CD133 and RET (RET9) on SH-SY5Y cells. RET-expressing lentivirus was co-infected into stably CD133-expressing SH-SY5Y cells. Ten days after infection, ectopic RET and CD133 expressions were observed both at protein

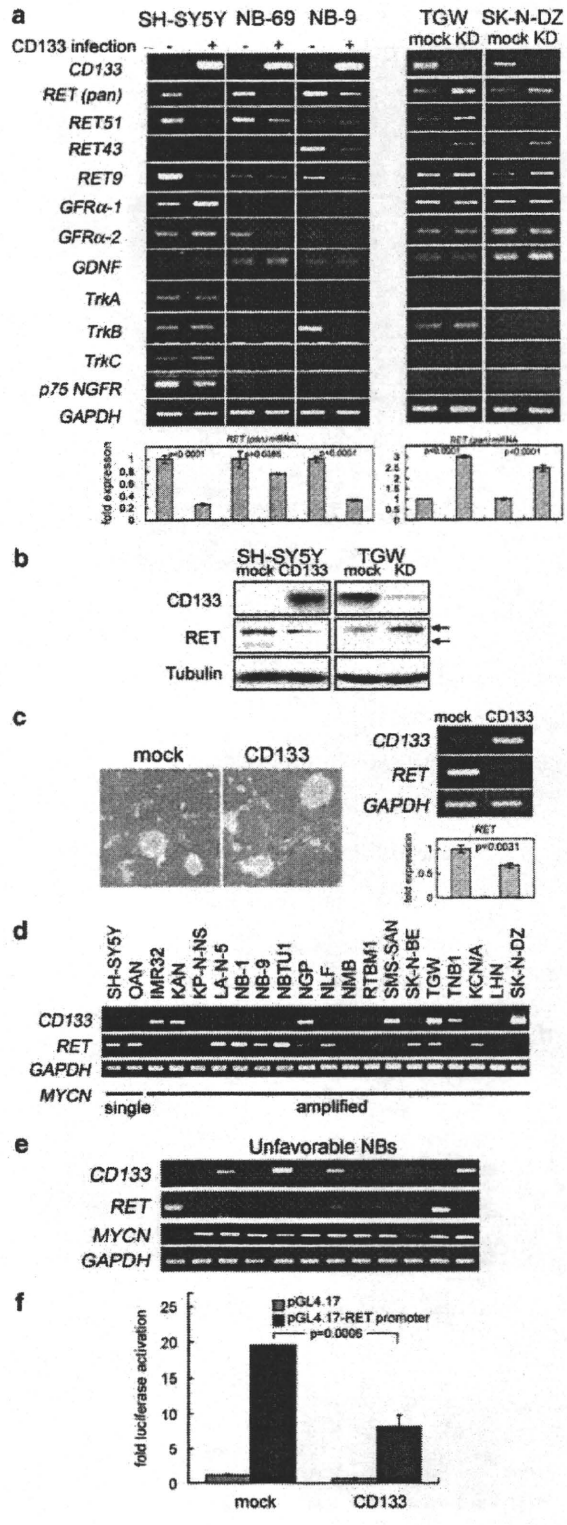

Figure 3 CD133 inhibits RET expression in NB cells. (**a**) SH-SY5Y, NB-69 and NB-9 cells were infected with mock or CD133-expressing lentivirus, and TGW and SK-N-DZ cells were stably infected with shRNA against mock or CD133 (KD) lentivirus. Semi-quantitative RT–PCR analyses were performed with CD133-modified NBs using specific primers against each *RET* isoform, *Trk* families, *GFRα-1/2* and *GDNF*. *GAPDH* was used as a loading control. Expression level of *RET* (pan) was analyzed by qPCR. In qPCR, relative *RET* values were normalized by *GAPDH*. Data are representative results of at least three independent experiments. (**b**) CD133-expressing SH-SY5Y or CD133 knocked-down TGW cell lysates were subjected to western blotting for CD133 and pan-RET expression. Pan-RET antibody detected two bands corresponding to RET isoforms (arrows). (**c**) Primary sphere from a stage 4 NB patient was infected with mock or CD133-expressing lentivirus. Five days after infection, RNA was extracted for semi-quantitative RT–PCR of *CD133*/*RET* and qPCR of *RET*. GAPDH was used as an internal control. Data are representative of three tumor samples. (**d**) Expression of *CD133* and *RET* mRNA in NB cell lines. In all, 18 NB cell lines with amplified *MYCN* and 2 cell lines with a single copy of *MYCN* were used for semi-quantitative RT–PCR analysis. (**e**) Semi-quantitative RT–PCR analysis in unfavorable primary NBs. The results of 12 NBs are shown. Unfavorable NBs: International NB Staging System (INSS) stage 3 or 4, *TrkA* (−), with *MYCN* amplified. (**f**) Effects of CD133 on *RET* promoter (0.8 kb) activity in SH-SY5Y cells. pGL4.17-*RET* promoter-driven luciferase activities were normalized to pRL-SV40 early enhancer/promoter-driven *Renilla* luciferase activities as the transfection control and expressed as relative values.

and mRNA levels (Figure 4b and data not shown). As seen in Figure 4a, GDNF significantly induced neurite outgrowth of CD133/RET co-expressing SH-SY5Y cells. CD133 single-infected cells did not respond to GDNF, suggesting that the response was dependent on RET receptor expression. However, the expression of neuronal cell differentiation markers induced by GDNF was not recovered by *RET* in CD133-expressing cells (Figure 4b). These findings indicated that CD133 inhibits GDNF-promoted neuronal differentiation via not only by *RET* but also by the other signal pathways.

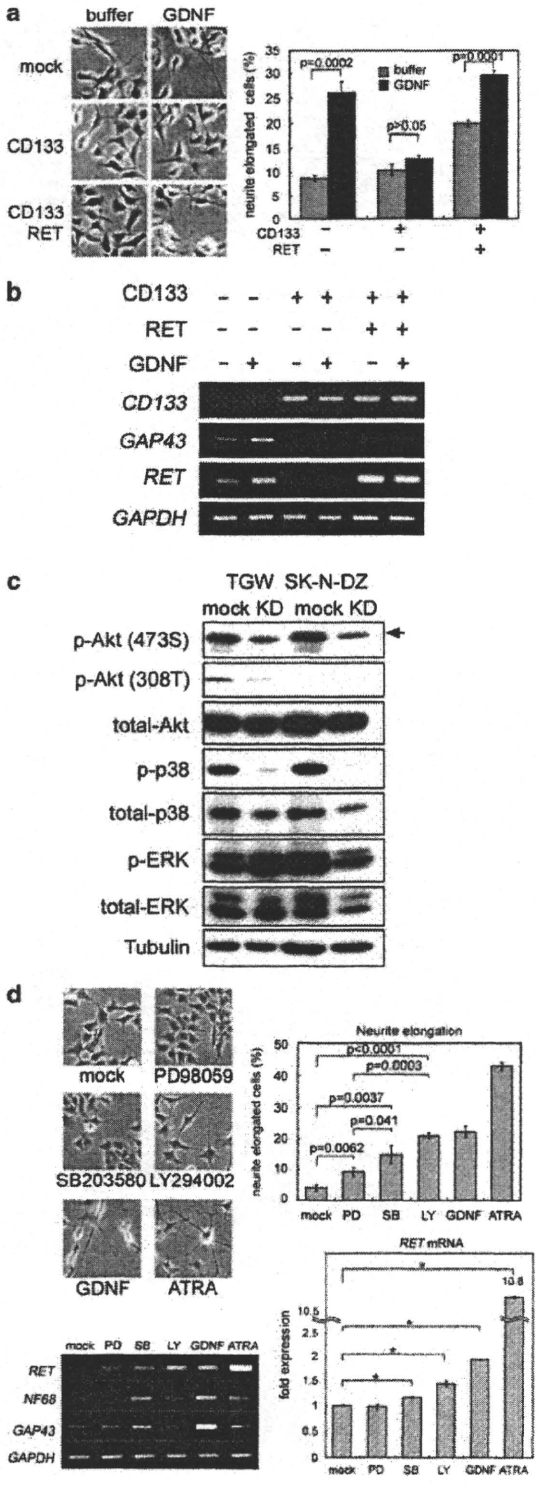

Figure 4 NB cell differentiation was regulated by CD133-dependent RET suppression via signal pathway modification. (**a**) Mock, CD133 and/or RET9 co-expressing SH-SY5Y cells were treated with GDNF (50 ng/ml) for 72 h. Cells were scored for the presence of neurites longer than one cell diameter after GDNF treatment. (**b**) CD133 and/or RET9 co-infected SH-SY5Y cells were cultured with or without GDNF treatment. Semi-quantitative RT–PCR analyses of *CD133*, *GAP43*, *RET* and *GAPDH* were performed. (**c**) The levels of phospho-Akt (p-Akt(473S) and p-Akt(308 T)), total-Akt, phospho-p38MAPK (p-p38), total-p38MAPK, phospho-ERK (p-ERK), total-ERK and tubulin were analyzed by western blot analysis. (**d**) TGW cells were cultured with DMSO (mock, 0.1%), PD98059 (PD, 5 μM), SB203580 (SB, 5 μM), LY294002 (LY, 5 μM), GDNF (50 ng/ml) or ATRA (5 μM) for 96 h. Cells were scored for the presence of neurite longer than one cell diameter after treatments. Semi-quantitative RT–PCR analysis of *RET*/*NF68*/*GAP43*/*GAPDH*, and qPCR of *RET* were performed.

CD133 regulates RET expression and NB cell differentiation by modification of signaling pathways

To identify the mechanism of *RET* downregulation in CD133-expressing cells, we studied the signaling molecule status in CD133 knocked-down cells (Figure 4c) and found a strong suppression of Akt (473S, 308T) and p38MAPK phosphorylation, but not ERK1/2 in both TGW and SK-N-DZ cells. To confirm the Akt and p38MAPK phosphorylation status caused by CD133 downregulation, we treated TGW cells with kinase inhibitors. MEK1 inhibitor (PD98059, PD), p38MAPK inhibitor (SB203580, SB) and PI3K inhibitor (LY294002, LY) induced neurite elongation in NB cells, and SB and LY were more effective for neurite elongation than PD. *RET* induction by kinase inhibitors was correlated with neurite elongation; however, differentiation markers *NF68* and *GAP43* were significantly induced by SB treatment. These results suggest that downregulation of p38MAPK and PI3K/Akt pathways has a function in CD133-related neurite elongation and differentiation marker expression is affected mainly by the p38MAPK pathway.

CD133 has a function in tumor-sphere growth and cell survival

It was previously reported that NB TICs were accumulated in NB spheres in serum-free media (SFM) (Hansford *et al.*, 2007). These observations prompted us to study the function of CD133 in tumor-sphere formation of NB cells. In IMR32 cells, only a small fraction of cells expressed CD133 (Supplementary Figure 1Sa). IMR32 cells were cultured in SFM with epidermal growth factor and fibroblast growth factor for a week, and sphere formation, upregulation of *CD133* (11.8-fold induction) and suppression of *RET* (2.8-fold reduction) were observed (Figure 5a). In primary NB cells from bone marrow metastasis,

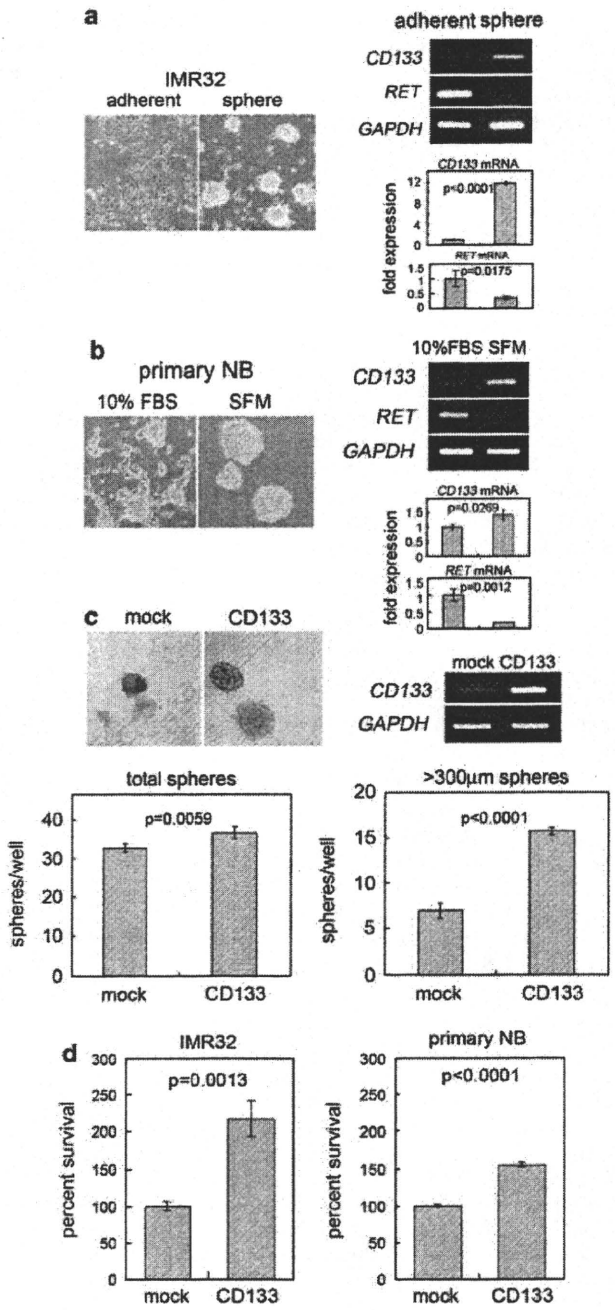

Figure 5 CD133 enhances cellular survival of NB cells in neurospheres. IMR32 cells (**a**) and primary NB cells (**b**) were cultured in 10% fetal bovine serum containing medium (adherent) or SFM (sphere) for a week. Semi-quantitative RT–PCR and qPCR analyses were performed with adherent or sphere cell RNAs using specific primers for *CD133* and *RET*. *GAPDH* was used as a loading control. Primary NB cell results are representative of three tumor samples. (**c**) IMR32 cells were stably infected with mock or CD133-expressing lentivirus. The expression levels of *CD133* and *GAPDH* were determined by semi-quantitative RT–PCR. Cells were cultured in 96-well culture plates with SFM. After 5 weeks, spheres were measured and counted under a microscope with an eyepiece micrometer. (**d**) Enzymatically dissociated IMR32- or primary NB-sphere cells were stained with trypan blue and counted to determine the number of viable cells.

the upregulation of CD133 (1.4-fold induction) and downregulation of RET receptors (5.9-fold reduction) were found in SFM medium, but not in the medium with 10% fetal bovine serum (Figure 5b). Next, we introduced CD133 into IMR32 cells by lentivirus infection, and after 5-week culture in SFM, we found that CD133-expressing cells formed many more large spheres than mock cells (Figure 5c). Moreover, CD133-expressing spheres made from IMR32 and primary NB cells contained many more living cells than the mock control (Figure 5d), suggesting that CD133 promotes NB cell survival in tumor-sphere formation.

Discussion

Increasing evidence highlights the function of CD133 as a marker of CSCs in various human tumors; however, its function in tumorigenesis remains to be elucidated by molecular biology experiments. In this study, CD133-knockdown experiments indicated that CD133 represses differentiation in NB cells; CD133 was clearly decreased by differentiation-inducing stimulation, for example ATRA and TPA treatments. Brodeur *et al.* (2000) indicated that neurotrophic factors and their receptors have a significant function in NB behavior and the potential to send intracellular signals into the nucleus to produce neuronal differentiation in the normal sympathetic nerve system. Among the NB cell differentiation-related neurotrophic receptors, *RET* transcription was regulated by CD133 in NB cell lines. The expression of CD133 effectively inhibited NB cell differentiation (neurite extension and differentiation markers). Furthermore, RET expression partly rescued the CD133-related inhibition of differentiation. These findings suggest that CD133-mediated RET suppression has a considerable function in NB cell differentiation. Regarding the function of RET in NB differentiation, Peterson and Bogenmann (2004) suggested that RET receptor activation inhibits cell cycle progression and enhances responsiveness to NGF; thus, NB cell differentiation requires the collaboration of functional RET and TrkA signal pathways; they also reported that GDNF treatment induced *RET* transcription in NB cells. Intriguingly, our results indicate that CD133 expression effectively suppressed *RET* mRNA in NB cells and CD133 knockdown induced NB cell differentiation, suggesting that suppression of CD133 by small-interference RNA administration will increase *RET* transcription in CD133-expressing NB tumors and may be useful in differentiation induction therapy for resistant- and relapsed-NB tumors. In addition, transcriptional suppression of *CD133* could be useful to induce differentiation in NB cells; however, the exact mechanism of transcriptional regulation of CD133 has not been clarified. Although seven CD133 mRNA isoforms controlled by five alternative promoters were reported previously (Shmelkov *et al.*, 2004), the promoter activities of these isoforms were studied only by pGL3-enhancer vector, suggesting the existence of other *cis*-elements in the CD133 locus.

Several studies have been reported to elucidate the molecular mechanism and signaling pathways that regulate the behavior of CD133-expressing cancer cells. Nikolova *et al.* (2007) reported that WNT-conditional media had effects on the proliferation and differentiation of cord blood-derived CD133-positive cells, and Fan *et al.* (2006) showed that Notch signal inhibition by GSI-18 reduced the CD133-positive fraction in brain tumor cells. Regarding the analysis of the intracellular signaling pathway related to the CD133 function, one report suggested the significance of the Akt/PKB pathway in the expression of survival proteins, phosphor-Bad and Bcl-2 in CD133-positive hepatocellular carcinoma cell survival (Ma *et al.*, 2007). In our study, CD133-knockdown experiments indicated that CD133-related RET repression and NB cell differentiation were caused by signal pathway activation, for example p38MAPK and PI3K/Akt pathways. To support this observation, treatment with kinase inhibitors showed a correlation between neurite elongation and RET induction in NB cells, and that differentiation marker protein induction was mainly dependent on the p38MAPK pathway. These findings suggest that CD133 prevents NB cell differentiation via signal transduction pathways. To the best of our knowledge, this is the first report of CD133-related signal pathway modification resulting in cell differentiation. As CD133 is a membranous protein on stem cells and cancer stem cells, it is possible that CD133 affects membranous receptor functions and the downstream signal pathways. In addition, Boivin *et al.* (2009) reported the phosphorylation of CD133-cytoplasmic tyrosine-828 and tyrosine-852 by Src and Fyn tyrosine kinases. Site-directed mutagenesis of these tyrosine residues in CD133 will provide important information for CD133 functions in our experimental system using NB cells.

Materials and methods

Cell culture and reagents
Human NB cell lines were obtained from official cell banks (RIKEN Cell Bank, Tsukuba, Japan and ATCC, Manassas, VA, USA) and cultured in high-glucose DMEM (Sigma-Aldrich, St Louis, MO, USA) or RPMI1640 (Wako, Osaka, Japan) supplemented with 10% heat-inactivated fetal bovine serum (Invitrogen, Carlsbad, CA, USA) and 50 μg/ml penicillin/streptomycin (Sigma-Aldrich) in an incubator with humidified air at 37 °C with 5% CO_2. NB cell lines subjected to molecular biology and biochemistry experiments were MYCN single-copy SH-SY5Y cells and MYCN-amplified TGW, SK-N-DZ and IMR32 cells. GDNF was obtained from Invitrogen. ATRA was from Sigma-Aldrich. Phorbol-12-myristate-13-acetate (TPA) was from Nacalai Tesque (Kyoto, Japan). LY294002 was from Cell Signaling Technology (Beverly, MA, USA). PD98059 and SB203580 were from Calbiochem (San Diego, CA, USA).

Fluorescence-activated cell sorting analysis
NB cell lines growing in the log phase were enzymatically removed from 10 cm diameter culture dishes, washed with cold PBS and treated with biotinylated AC133 (CD133/1) monoclonal antibodies (Miltenyi Biotec, Auburn, CA, USA) or control IgG2A (eBioscience, San Diego, CA, USA) for 15 min at 4 °C. The primary antibody was removed, and then the cells were washed twice with ice-cold PBS containing 0.1% BSA, and a 1:200 dilution of phycoerythrin-labeled streptavidin (eBioscience) added for 15 min at 4 °C. After washing, flow cytometry was performed using a fluorescence-activated cell sorting Caliber (BD, San Jose, CA, USA).

Knockdown of CD133
For RNAi experiments, predesigned, double-stranded SMART-pool small-interference RNA targeting human *CD133* (*prominin-1*) was purchased from Dharmacon (Lafayette, CO, USA) and Silencer Negative Control small-interference RNA #1 was purchased from Ambion (Austin, TX, USA).

Lentivirus-mediated gene transduction and knockdown
The packaging cell line HEK 293T (4×10^6) was plated and transfected the following day. Then, 1.5 μg transducing vectors containing the gene [pHR-SIN-CMV-G-DL1 or CSII-CMV-MCS-IRES2-Bsd vector (RIKEN Bioresource Center, Ibaraki, Japan)] or shRNA [pLKO.1 (Sigma-Aldrich)] and 2.0 μg packaging vectors (Sigma-Aldrich) were co-transfected with Fugene 6 transfection reagent (Roche Applied Science, Indianapolis, IN, USA) according to the manufacturer's protocols. The medium was changed the following day, and cells were cultured for another 24 h. Conditioned medium was collected and cleared of debris by filtering through a 0.45 μm filter (Millipore, Bedford, MA, USA). Then, 1×10^5 NB cells were seeded in each well of a six-well plate, and transduced by lentiviral-conditioned media. Transduced cells were analyzed by western blotting and RT–PCR.

Cloning of human CD133 cDNA
The human *CD133* cDNA (RefSeq NM_006017) was cloned from human colon cancer cell line Caco-2 mRNA by RT–PCR using specific primer sets described in Supplementary Table 1S. *CD133* cDNA fragment was sub-cloned into a lentiviral-based vector (pHR-SIN-CSGW) (Hasegawa *et al.*, 2006).

Western blot analysis
The cells were lysed in buffer containing 5 mM EDTA, 2 mM Tris–HCl (pH 7.5), 10 mM β-glycerophosphate, 5 μg/ml aprotinin, 2 mM phenylmethylsulfonyl fluoride, 1 mM Na_3VO_4, a protease inhibitor cocktail (Nacalai Tesque) and 1% SDS. Western blot analysis was performed as reported previously (Kurata *et al.*, 2008). For CD133 detection, we used AC133 monoclonal antibody. Anti-RET (Santa Cruz Biotechnology, Santa Cruz, CA, USA), anti-phospho- and total Akt, p38, ERK (Cell Signaling Technology) and anti-tubulin antibody from Lab Vision (Fremont, CA, USA) were also used.

Semi-quantitative RT–PCR
Semi-quantitative RT–PCR analysis was as described previously (Kurata *et al.*, 2008). Total cellular RNA for preparing RT–PCR templates was extracted using ISOGEN (Nippon Gene KK, Tokyo, Japan). The cDNA was synthesized from 1 μg total RNA and then subjected to PCR. Primer sequences are described in Supplementary Table 1S. RT–PCR results are representative of at least three independent experiments.

qPCR analysis
The qPCR analysis was performed as described previously (Ochiai *et al.*, 2010). The primers for qPCR were designed and synthesized to produce 50–150 bp products. The primer sequence is listed in Supplementary Table 1S. The results were representative of at least three independent experiments.

Cell proliferation and soft agar assay
Cells were seeded into 96-well plates (750 per well) in culture medium containing 10% fetal bovine serum. Every 24 h, cell viability was determined by water-soluble tetrazolium salt (WST-8) assay using Counting kit-8 (Dojindo, Kumamoto, Japan) according to the manufacturer's protocol. For soft agar assay, 2×10^3 cells of stable infectants TGW or SH-SY5Y cells were seeded in soft agar as described previously (Aoyama *et al.*, 2005). Viable colonies were stained with 0.05 mg/ml MTT.

Tumor formation in nude mice
For tumor formation, 6-week-old female athymic BALB/c AJcl *nu/nu* mice (CLEA Japan, Shizuoka, Japan) were injected into the femur with 1×10^7 TGW cells as described previously (Aoyama *et al.*, 2005). The handling of animals was in accordance with the guidelines of Chiba Cancer Center Research Institute.

Patients and tumor specimens
The 12 tumor specimens used in this study were kindly provided by various institutions and hospitals in Japan. Informed consent was obtained at each institution or hospital. All tumors were diagnosed clinically as well as pathologically as NB and staged according to the International NB Staging System criteria. The patients were treated by standard chemotherapy protocols as described previously (Kaneko *et al.*, 2002; Iehara *et al.*, 2006). *MYCN* copy number, *TrkA* mRNA expression levels and DNA index were measured as reported previously (Ohira *et al.*, 2003). This study was approved by the Institutional Review Board of Chiba Cancer Center.

Subcloning of human RET (RET9)
Human *RET9* (Crowder *et al.*, 2004) full-length cDNA was a kind gift from Dr Hideki Enomoto (RIKEN Center for Developmental Biology, Hyogo, Japan). *RET9* cDNA fragment (3.4 kb) was sub-cloned into the *Not*I site of CSII-CMV-MCS-IRES2-Bsd vector, which had been altered to accept the *Xba*I and *Hin*dIII ends.

Cloning of human RET promoter
Human *RET* promoter 1.5 kb (−919 to +550, position +1 is the transcription start site determined in a previous report (Itoh *et al.*, 1992)) was amplified from human genomic DNA using Platinum *Pfx* polymerase (Invitrogen) with primers (described in Supplementary Table 1S) by PCR amplification and sub-cloned into pGEM-T easy vector (Promega, Southampton, UK). The *RET* 5′-flanking sequence from −453 to +227 was sub-cloned into the *Eco*RV site of pGL4.17 reporter vector (Promega).

Sphere culture of NB cells
The preparation of primary NB cells from stage 4 patients' bone marrow was described previously (Nakanishi *et al.*, 2007). Dissociated primary NB cells or IMR32 cells were cultured in SFM (DMEM-F12, 1:1 (Wako), 50 μg/ml penicillin/streptomycin, 2% B27 supplement (Invitrogen), 20 ng/ml epidermal growth factor (Sigma-Aldrich) and 20 ng/ml fibroblast growth factor basic (Invitrogen)). Half of the medium was replaced with fresh culture medium every 7 days. IMR32 cells and primary NB cells were seeded in 96-well (400 per well) or six-well (1×10^5 per well) and six-well (1.7×10^5 per well) plates, respectively. Spheres were counted and measured under a microscope with an eyepiece micrometer. Five-week cultured IMR32 or 2-month cultured primary NB spheres were dissociated by Accumax (Innovative Cell Technologies, San Diego, CA, USA) according to the manufacturer's protocol. Living cells were counted based on morphological criteria and trypan blue staining.

Conflict of interest

The authors declare no conflict of interest.

Acknowledgements

We thank K Sakurai and S Matsushita for technical assistance, Dr Hiroyuki Miyoshi (BioResource Center, RIKEN) for the gift of CSII-CMV-MCS-IRES2-Bsd plasmid and Daniel Mrozek, Medical English Service, for editorial assistance. This work was supported in part by a grant-in-aid from JSPS for Young Scientists (B) (number: 19790274), a grant-in-aid from the Ministry of Health, Labor, and Welfare for Third Term Comprehensive Control Research for Cancer, a grant-in-aid for Cancer Research (20–13) from the Ministry of Health, Labor, and Welfare of Japan and a grant-in-aid from the Ministry of Education, Culture, Sports, Science and Technology, Japan (number: 21591377).

References

Aoyama M, Ozaki T, Inuzuka H, Tomotsune D, Hirato J, Okamoto Y *et al.* (2005). LMO3 interacts with neuronal transcription factor, HEN2, and acts as an oncogene in neuroblastoma. *Cancer Res* **65**: 4587–4597.

Boivin D, Labbé D, Fontaine N, Lamy S, Beaulieu E, Gingras D *et al.* (2009). The stem cell marker CD133 (prominin-1) is phosphorylated on cytoplasmic tyrosine-828 and tyrosine-852 by Src and Fyn tyrosine kinases. *Biochemistry* **48**: 3998–4007.

Brodeur GM, Sawada T, Tsuchida Y, Voute PA (eds) (2000). *Neuroblastoma*. Elsevier Science: Amsterdam.

Collins AT, Berry PA, Hyde C, Stower MJ, Maitland NJ. (2005). Prospective identification of tumorigenic prostate cancer stem cells. *Cancer Res* **65**: 10946–10951.

Corbeil D, Roper K, Hellwig A, Tavian M, Miraglia S, Watt SM *et al.* (2000). The human AC133 hematopoietic stem cell antigen is also expressed in epithelial cells and targeted to plasma membrane protrusions. *J Biol Chem* **275**: 5512–5520.

Corbeil D, Fargeas CA, Huttner WB. (2001). Rat prominin, like its mouse and human orthologues, is a pentaspan membrane glycoprotein. *Biochem Biophys Res Commun* **285**: 939–944.

Crowder RJ, Enomoto H, Yang M, Johnson Jr EM, Milbrandt J. (2004). Dok-6, a Novel p62 Dok family member, promotes Ret-mediated neurite outgrowth. *J Biol Chem* **279**: 42072–42081.

D'Alessio A, De Vita G, Calì G, Nitsch L, Fusco A, Vecchio G *et al.* (1995). Expression of the RET oncogene induces differentiation of SK-N-BE neuroblastoma cells. *Cell Growth Differ* **6**: 1387–1394.

Enomoto H, Crawford PA, Gorodinsky A, Heuckeroth RO, Johnson Jr EM, Milbrandt J. (2001). RET signaling is essential for migration, axonal growth and axon guidance of developing sympathetic neurons. *Development* **128**: 3963–3974.

Enomoto H, Heuckeroth RO, Golden JP, Johnson EM, Milbrandt J. (2000). Development of cranial parasympathetic ganglia

requires sequential actions of GDNF and neurturin. *Development* **127**: 4877–4889.

Fan X, Matsui W, Khaki L, Stearns D, Chun J, Li YM *et al.* (2006). Notch pathway inhibition depletes stem-like cells and blocks engraftment in embryonal brain tumors. *Cancer Res* **66**: 7445–7452.

Hansford LM, McKee AE, Zhang L, George RE, Gerstle JT, Thorner PS *et al.* (2007). Neuroblastoma cells isolated from bone marrow metastases contain a naturally enriched tumor-initiating cell. *Cancer Res* **67**: 11234–11243.

Hasegawa K, Nakamura T, Harvey M, Ikeda Y, Oberg A, Figini M *et al.* (2006). The use of a tropism-modified measles virus in folate receptor-targeted virotherapy of ovarian cancer. *Clin Cancer Res* **12**: 6170–6178.

Itoh F, Ishizaka Y, Tahira T, Yamamoto M, Miya A, Imai K *et al.* (1992). Identification and analysis of the *ret* proto-oncogene promoter region in neuroblastoma cell lines and medullary thyroid carcinomas from MEN2A patients. *Oncogene* **7**: 1201–1206.

Iehara T, Hosoi H, Akazawa K, Matsumoto Y, Yamamoto K, Suita S *et al.* (2006). MYCN gene amplification is a powerful prognostic factor even in infantile neuroblastoma detected by mass screening. *Br J Cancer* **94**: 1510–1515.

Jordan CT, Guzman ML, Noble M. (2006). Cancer stem cells. *N Engl J Med* **355**: 1253–1261.

Kaplan D, Matsumoto K, Lucarelli E, Thiele CJ. (1993). Induction of TrkB by retinoic acid mediates biologic responsiveness to BDNF and differentiation of human neuroblastoma cells. Eukaryotic Signal Transduction Group. *Neuron* **11**: 321–331.

Kaneko M, Tsuchida Y, Mugishima H, Ohnuma N, Yamamoto K, Kawa K *et al.* (2002). Intensified chemotherapy increases the survival rates in patients with stage 4 neuroblastoma with MYCN amplification. *J Pediatr Hematol Oncol* **24**: 613–621.

Klein R. (1994). Role of neurotrophins in mouse neuronal development. *FASEB J* **8**: 738–744.

Kurata K, Yanagisawa R, Ohira M, Kitagawa M, Nakagawara A, Kamijo T. (2008). Stress via p53 pathway causes apoptosis by mitochondrial Noxa upregulation in doxorubicin-treated neuroblastoma cells. *Oncogene* **27**: 741–754.

Ma S, Lee TK, Zheng BJ, Chan KW, Guan XY. (2007). CD133+ HCC cancer stem cells confer chemoresistance by preferential expression of the Akt/PKB survival pathway. *Oncogene* **27**: 1749–1758.

Maris JM, Hogarty MD, Bagatell R, Cohn SL. (2007). Neuroblastoma. *Lancet* **369**: 2106–2120.

Maw MA, Corbeil D, Koch J, Hellwig A, Wilson-Wheeler JC, Bridges RJ *et al.* (2000). A frameshift mutation in prominin (mouse)-like 1 causes human retinal degeneration. *Hum Mol Genet* **9**: 27–34.

Miki J, Furusato B, Li H, Gu Y, Takahashi H, Egawa S *et al.* (2007). Identification of putative stem cell markers, CD133 and CXCR4, in hTERT-immortalized primary nonmalignant and malignant tumor derived human prostate epithelial cell lines and in prostate cancer specimens. *Cancer Res* **67**: 3153–3161.

Monzani E, Facchetti F, Galmozzi E, Corsini E, Benetti A, Cavazzin C *et al.* (2007). Melanoma contains CD133 and ABCG2 positive cells with enhanced tumourigenic potential. *Eur J Cancer* **43**: 935–946.

Myers SM, Eng C, Ponder BA, Mulligan LM. (1995). Characterization of RET proto-oncogene 3′ splicing variants and polyadenylation sites: a novel C-terminus for RET. *Oncogene* **11**: 2039–2045.

Nakanishi H, Ozaki T, Nakamura Y, Hashizume K, Iwanaka T, Nakagawara A. (2007). Purification of human primary neuroblastomas by magnetic beads and their *in vitro* culture. *Oncol Rep* **17**: 1315–1320.

Nikolova T, Wu M, Brumbarov K, Alt R, Opitz H, Boheler KR *et al.* (2007). WNT-conditioned media differentially affect the proliferation and differentiation of cord blood-derived CD133+ cells *in vitro*. *Differentiation* **75**: 100–111.

O'Brien CA, Pollett A, Gallinger S, Dick JE. (2007). A human colon cancer cell capable of initiating tumour growth in immunodeficient mice. *Nature* **445**: 106–110.

Ochiai H, Takenobu H, Nakagawa A, Yamaguchi Y, Kimura M, Ohira M *et al.* (2010). Bmi1 is a MYCN target gene that regulates tumorigenesis through repression of *KIF1Bβ* and *TSLC1* in neuroblastoma. *Oncogene* **29**: 2681–2690.

Ohira M, Morohashi A, Inuzuka H, Shishikura T, Kawamoto T, Kageyama H *et al.* (2003). Expression profiling and characterization of 4200 genes cloned from primary neuroblastomas: identification of 305 genes differentially expressed between favorable and unfavorable subsets. *Oncogene* **22**: 5525–5536.

Olempska M, Eisenach PA, Ammerpohl O, Ungefroren H, Fandrich F, Kalthoff H. (2007). Detection of tumor stem cell markers in pancreatic carcinoma cell lines. *Hepatobiliary Pancreat Dis Int* **6**: 92–97.

Peterson S, Bogenmann E. (2004). The RET and TRKA pathways collaborate to regulate neuroblastoma differentiation. *Oncogene* **23**: 213–225.

Reya T, Morrison SJ, Clarke MF, Weissman IL. (2001). Stem cells, cancer, and cancer stem cells. *Nature* **414**: 105–111.

Ricci-Vitiani L, Lombardi DG, Pilozzi E, Biffoni M, Todaro M, Peschle C *et al.* (2007). Identification and expansion of human colon-cancer initiating cells. *Nature* **445**: 111–115.

Shmelkov SV, Jun L, St Clair R, McGarrigle D, Derderian CA, Usenko JK *et al.* (2004). Alternative promoters regulate transcription of the gene that encodes stem cell surface protein AC133. *Blood* **103**: 2055–2061.

Singh SK, Hawkins C, Clarke ID, Squire JA, Bayani J, Hide T *et al.* (2004). Identification of human brain tumour initiating cells. *Nature* **432**: 396–401.

Walton JD, Kattan DR, Thomas SK, Spengler BA, Guo HF, Biedler JL *et al.* (2004). Characteristics of stem cells from human neuroblastoma cell lines and in tumors. *Neoplasia* **6**: 838–845.

Weinberg RA (ed) (2006). *The Biology of Cancer*. Garland Science: New York.

Yin AH, Miraglia S, Zanjani ED, Almeida-Porada G, Ogawa M, Leary AG *et al.* (1997). AC133, a novel marker for human hematopoietic stem and progenitor cells. *Blood* **90**: 5002–5012.

Yin S, Li J, Hu C, Chen X, Yao M, Yan M *et al.* (2007). CD133 positive hepatocellular carcinoma cells possess high capacity for tumorigenicity. *Int J Cancer* **120**: 1444–1450.

Zacchigna S, Oh H, Wilsch-Bräuninger M, Missol-Kolka E, Jászai J, Jansen S *et al.* (2009). Loss of the cholesterol-binding protein prominin-1/CD133 causes disk dysmorphogenesis and photoreceptor degeneration. *J Neurosci* **29**: 2297–2308.

Supplementary Information accompanies the paper on the Oncogene website (http://www.nature.com/onc)

Journal of Pediatric Surgery (2010) 45, 2293–2298

ELSEVIER

Journal of Pediatric Surgery

www.elsevier.com/locate/jpedsurg

PAPS Papers

Reevaluation of *trkA* expression as a biological marker of neuroblastoma by high-sensitivity expression analysis—a study of 106 primary neuroblastomas treated in a single institute☆

Tomoro Hishiki[a,*], Takeshi Saito[a], Keita Terui[a], Yoshiharu Sato[a], Ayako Takenouchi[a], Eriko Yahata[a], Sachie Ono[a], Akira Nakagawara[b], Takehiko Kamijo[b], Yohko Nakamura[b], Tadashi Matsunaga[a], Hideo Yoshida[a]

[a]*Department of Pediatric Surgery, Chiba University Graduate School of Medicine, Chiba 260-8677, Japan*
[b]*Division of Biochemistry and Molecular Carcinogenesis, Chiba Cancer Center Research Institute, Chiba 260-8717, Japan*

Received 27 July 2010; accepted 12 August 2010

Key words:
Neuroblastoma;
trkA;
Quantitative PCR;
Real-time PCR

Abstract

Background/Purpose: It has previously been shown that neuroblastomas with favorable prognosis often express a high level of nerve growth factor receptor *trkA*. We performed an expression analysis of *trkA* in 106 NB samples based on the quantitative real-time polymerase chain reaction (PCR) and reevaluated the prognostic power of *trkA*.

Materials and methods: A total of 106 primary tumors from NB patients treated from 1988 to 2009 were analyzed. *MYCN* was amplified in 13 cases. TaqMan probe method was used for quantitative PCR. Primers and probes were designed to detect *trkA* I and *trkA* II, but not the oncogenic splice variant *trkA* III.

Results: Expression analysis by real-time PCR revealed a wide range of expression levels of *trkA* within neuroblastoma tissues. Extremely low levels of *trkA* that were undetectable by semiquantitative PCR were able to be quantified by this method. *trkA* was predominantly expressed in tumors with favorable outcome. Further analysis of *trkA* expression was performed in a cohort excluding mass-screened neuroblastomas. Strikingly, multivariate analysis containing age, *MYCN* status, and *trkA* expression identified *trkA* as the only variable that independently predicts the prognosis of the 44 patients who presented clinically.

Conclusion: High-resolution expression analysis targeting *trkA* and *trkA* II may add more statistical power on *trkA* as a biological marker.

☆ Sponsor: Prof Hideo Yoshida, Department of Pediatric Surgery, Chiba University Graduate School of Medicine.

* Corresponding author. Department of Pediatric Surgery, Chiba University Hospital, Chiba 260-8677, Japan. Tel.: +81 43 226 2312; fax: +81 43 226 2366.
E-mail address: hishiki@faculty.chiba-u.jp (T. Hishiki).

0022-3468/$ – see front matter © 2010 Elsevier Inc. All rights reserved.
doi:10.1016/j.jpedsurg.2010.08.021

Neuroblastoma is one of the most common extracranial solid tumors in children and originates from the sympathoadrenal lineage derived from the neural crest [1]. The prognosis of neuroblastoma patients older than 1 year tends to be poor, whereas that of patients younger than 1 year is usually favorable, with tumors having a potential to differentiate or to regress spontaneously [2]. Previous studies have shown that the biological behavior of neuroblastomas is strongly regulated by neurotrophins and their receptors [3]. *trkA* encodes the high-affinity receptor of nerve growth factor (NGF) and is predominantly expressed in neuroblastomas with favorable prognosis [4-11]. Primary culture studies have shown that NGF induces terminal differentiation of favorable neuroblastomas in vitro, suggesting that NGF signals regulate differentiation and growth arrest of *trkA*-expressing neuroblastomas [3,12]. However, in a recent study, Tacconelli and colleagues [13] demonstrated that a novel splice variant of *trkA*, in which exons 6, 7, and 9 are deleted, yields a product that lacks the functional extracellular IG-C1 and N-glycosylation domains, and exhibits spontaneous tyrosine kinase activity that leads to oncogenic signals. In contrast to the previously known isoforms *trkA* I and *trkA* II, this newly identified product, named *trkA* III, is unresponsive to NGF, and antagonizes the differentiation/regression signals of NGF/TrkA.

The quantitative TaqMan real-time polymerase chain reaction (PCR) system determines the initial copy number of the target gene by a kinetic analysis of the cycle-to-cycle change in the fluorescence signal as a result of the amplification of the template during PCR. The method has gained reliability in highly sensitive quantification of genomic copies and mRNA expression in diverse fields of biology. The aim of this study was to analyze the expression of *trkA* in neuroblastomas using this highly dependable method and to reevaluate the prognostic significance of *trkA* expression in neuroblastomas treated in a single institute. The analysis was designed to detect the nononcogenic *trkA* I and *trkA* II, but not *trkA* III.

1. Materials and methods

1.1. Patients and treatment

The 106 patients with neuroblastomas analyzed were treated at the Chiba University Hospital from 1988 to 2008. The median follow-up period after diagnosis for the surviving children was 137 months (range, 13-251 months). The patients were staged according to the International Neuroblastoma Staging System (INSS) [14]. Of the 106 cases, 30 were diagnosed at an age older than 365 days and the remaining 76 were younger than 365 days; 62 of the 76 infantile patients were identified by the Japanese Neuroblastoma Mass Screening System [15]. Patients were treated mainly following the Japanese study group protocols for neuroblastoma [16,17].

1.2. Real-time quantitative reverse transcriptase-PCR

Written informed consent was obtained for the laboratory analysis according to the institutional requirements before the surgery. Total cytoplasmic RNA (5 μg) extracted from tumor samples was reverse transcribed using Ready-To-Go You-Prime First-Strand Beads (GE Healthcare UK Ltd, Amersham Place, England) and random hexanucleotide primers. Primers and probes for the real-time quantitative PCR were designed based on the Universal Probe Library. The sequences of primers and probes were as follows: *trkA*—forward primer, 5′-TGCAGTGTCATGGGCAAG-3′; reverse primer, 5′-GAGAAGGGGATGCACCAGT-3′; TaqMan probe, Universal probe library no. 45; GAPDH—forward primer, 5′-AGCCACATCGCTCAGACA-3′; reverse primer, 5′-GCCCAATACGACCAAATCC-3′; TaqMan probe, Universal probe library no. 60. The primer set for *trkA* flanks exons 6 and 7, and probe no. 45 hybridizes within exon 7. As a result, the system solely detects the expression of *trkA* I and *trkA* II, but not the oncogenic *trkA* III, in which exons 6 and 7 are deleted [13]. Light Cycler Real-time PCR system (Roche Applied Science, Tokyo, Japan) was used for quantitative PCR. Reactions were performed in a final volume 25 μL, and each sample was analyzed in duplicate. Each reaction mixture contained 0.1 pmol/μL Universal probe, 0.2 pmol/μL each primer, 1 × TaqMan PCR master mix, and 16.5 ng DNA. Thermal cycling was initiated with a denaturation step of 10 min at 95°C and then 40 cycles of 2-step PCR consisting of 95°C for 5 seconds and 60°C for 1 minute.

1.3. *MYCN* amplification and DNA ploidy

Amplification of *MYCN* was quantified by either Southern blot analysis or real-time PCR according to the previously described methods [18]. Tumors with *MYCN* gene amplification of 10 copies and more were categorized as *MYCN*-amplified tumors. DNA ploidy was assessed by FACS analysis calculating the ratio of propidium iodide fluorescence of the tumor cells against normal control.

1.4. Statistical analysis

Comparison of *trkA*/GAPDH ratio among 2 stratified groups (alive and well vs dead, *MYCN* amplified vs nonamplified, age younger than 1 year vs older 1 year, diploid vs nondiploid, favorable histology vs unfavorable histology) was performed by Wilcoxon rank test. Correlation between *trkA* and age was analyzed by Spearman rank correlation test. Survival curves were constructed according to the methods of Kaplan and Meier, and comparisons of the survival curves were performed with a log-rank test. Multivariate analyses were performed with the use of a Cox proportional-hazards regression model to identify

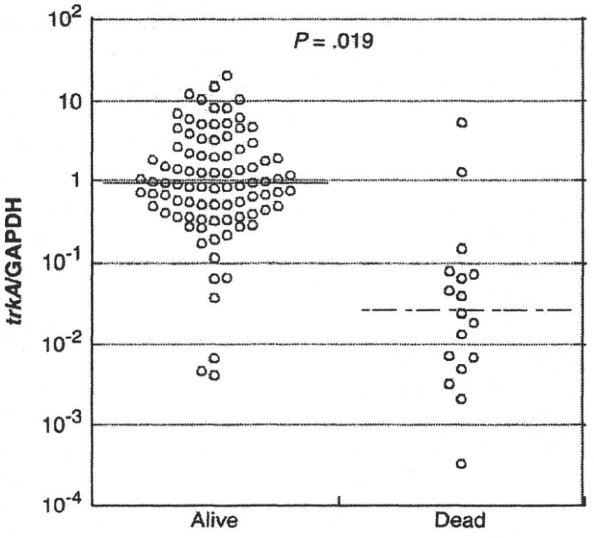

Fig. 1 Expression of *trk*A in alive and dead patients.

variables that were independently predictive of outcome. All statistical analysis was reviewed by a medical statistician (referred in Acknowledgments).

2. Results

2.1. Expression of *trkA* in primary neuroblastomas via quantitative PCR

The expression of *trkA*, excluding its oncogenic isoform *trkA* III, was assessed in 106 primary neuroblastoma samples. All samples were normalized by the expression of GAPDH using the corresponding cDNAs. The results of *trkA* expression are thus shown in the ratio of *trkA*/GAPDH. The PCR ratio ranged from 3.26×10^{-4} to 1.98×10^{2} (median, 0.753). The patients who were alive and well doing (n = 89; median *trkA*/GAPDH ratio, 0.94) expressed significantly higher levels of *trkA* compared to those who died (n = 17; median *trkA*/GAPDH ratio, 0.02) (Fig. 1; $P = .019$).

2.2. Expression of *trkA* and correlation to known prognostic factors

Younger patients had tumors with significantly higher expression of *trkA* (Spearman rank correlation test; $P = .028$: data not shown). Among the patients younger than 12 months, 72 (94.7%) of 76 tumors showed high *trkA* expression (*trkA*/GAPDH ratio >0.1), whereas in patients older than 12 months at diagnosis, only 14 (46.7%) of 30 tumors had high *trkA* expression. Low-staged tumors predominantly expressed high levels of *trkA*, whereas advanced staged and metastatic cases expressed lower levels of *trkA* (median *trkA*/GAPDH ratio; stage 1, 1.25 [n = 43], stage 2, 0.98 [n = 24], stage 4S, 0.75 [n = 6], stage 3, 0.27 [n = 8], stage 4, 0.039 [n = 25]) (Fig. 2). Stage 1, 2 and 4S tumors expressed statistically higher levels of *trkA* compared with stage 3 and 4 tumors ($P < .001$). *MYCN* gene amplification also had a strong inverse relationship with *trkA* expression (Fig. 2, $P = .015$). *MYCN* nonamplified tumors expressed significantly higher levels of *trkA* (n = 93; median *trkA*/GAPDH ratio, 0.94) compared to amplified tumors (n = 13; median *trkA*/GAPDH ratio, 0.015).

Among the 106 cases analyzed, DNA ploidy and histopathology (Shimada category) were assessed in 57 cases. Diploid tumors express lower levels *trkA* (n = 13; median *trkA*/GAPDH ratio, 0.13), whereas nondiploid tumors significantly expressed higher levels of *trkA* (n = 44; median *trkA*/GAPDH ratio, 0.80) (Fig. 2; $P = .011$). Regarding histopathology, tumors with favorable histology expressed significantly higher levels of *trkA* (n = 48; median *trkA* /GAPDH ratio, 0.85) compared with unfavorable

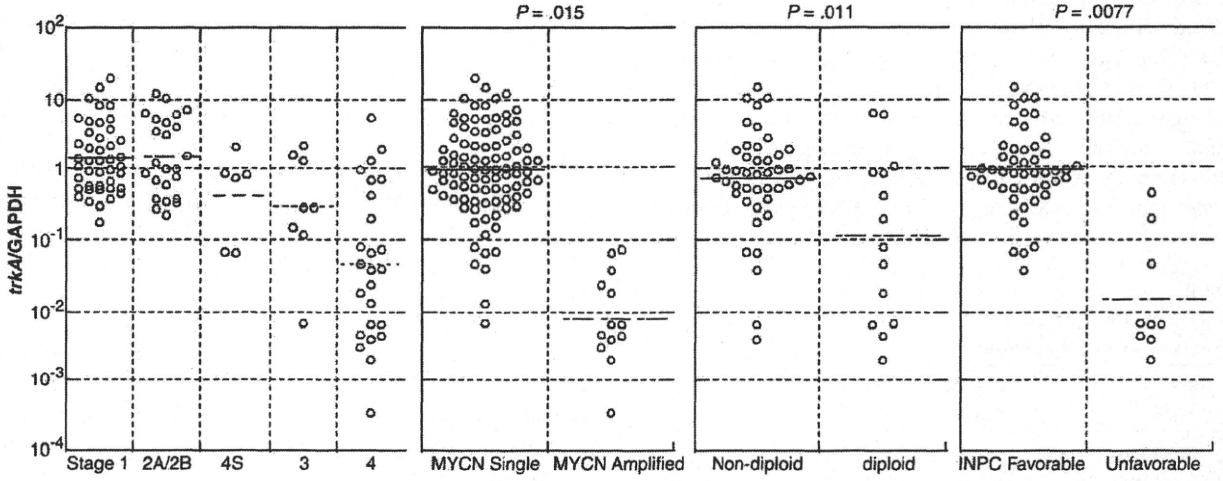

Fig. 2 Expression of *trk*A in *MYCN* nonamplified and amplified neuroblastomas, INSS stage groups, diploid and nondiploid tumors, and favorable/unfavorable histopathology categories.

Table 1 Results of univariate analysis of overall survival in 44 neuroblastoma patients presenting clinically

Variables	No of patients	3 yr overall survival (%)	*P*
MYCN status			.005
Nonamplified	31	80.9	
Amplified	13	44.9	
Age			<.001
<365 days	16	100	
≥365 days	28	55.9	
trkA / GAPDH ratio			<.001
≥median	22	94.7	
<median	22	47.1	
Stage			<.001
1, 2, or 4S	16	100	
3 or 4	28	55.9	
Shimada histopathologic category			.0173
Favorable	16	93.3	
Unfavorable	13	51.9	
DNA ploidy			.0046
Diploid	9	47.6	
Others	17	94.1	

tumors (n = 9; median *trkA* /GAPDH ratio, 0.0066) (Fig. 2; $P = .0077$).

2.3. Prognostic value of *trkA* in clinically presented neuroblastomas

The cohort of the current study included 62 cases that were detected by the Japanese Neuroblastoma Mass Screening System, which are known to have a very good prognosis. To assess the true prognostic value of *trkA* on an internationally comparable basis, we further excluded the cases detected by mass screening from the analysis and evaluated the expression of *trkA* in the 44 cases that presented clinically. Univariate analysis of previously known prognostic factors, along with the expression of *trkA* (below and over the median PCR ratio) was analyzed by comparing the survival curves of each variable using log-rank test. The results are shown in Table 1. *MYCN* amplification, age of 365 days or older, *trkA*/GAPDH ratio less than median, INSS stage 3 or 4, Shimada histopathologic category unfavorable, and diploid tumors were all identified as significant predictors of poor prognosis. Next, Cox proportional hazard test was carried out to clarify the independent impact of each factor on the prognosis of the 44 patients presenting clinically. The results of proportional hazard models are listed in Table 2. Among *MYCN* status, age, and *trkA* expression, only low *trkA* expression was identified to independently predict poor prognosis (Table 2; $P = .0071$). *MYCN* amplification and age older than 1 year were no longer significant. Clinical stage was not assessable in this series because there were no deaths in stage 1, 2, and 4S category. In addition, within the 26 cases in which data for Shimada histopathology category and DNA ploidy were available, there were no deaths in both the high *trkA* expression group and the younger age group (<365 days). Therefore, it was not possible to perform multivariate analysis containing histopathology and DNA ploidy as variables.

Table 2 Results of Multivariate Cox Model of Overall survival for age, *MYCN* status and *trkA* expression in 44 clinically detected neuroblastoma cases

Variables	Hazard Ratio	95% Confidence Interval	*P*
Age >365 days	6.220	0.801-48.296	.0805
MYCN amplified	1.190	0.415-3.409	.7461
trkA / GAPDH <median	9.204	1.826-46.381	.0071

3. Discussion

trkA as a prognostic factor of neuroblastoma was reevaluated using a highly sensitive expression analysis in the present study. Our results reconfirm the previous reports that the expression of *trkA* has statistical power to predict the patient's prognosis, and furthermore suggest that high-quality analysis of *trkA* expression, particularly of the *trkA* I and II isoforms, may add more statistical power compared to the previous *trkA* expression analyses [9-11,19].

Among the previous reports in which *trkA* expression in neuroblastomas were studied, early studies measured the expression mainly by Northern blot analysis or semiquantitative PCR [4-6,9]. The advantage of real-time PCR compared to these methods is speed, as well as sensitivity and accurate quantification. Particularly, TaqMan real-time PCR method yields high specificity compared to SYBR green real-time PCR method because of the minimum risk of nonspecific detection of amplified targets. The range of *trkA* expression detected by TaqMan real-time PCR was by far wider compared with that of our previous study performed by semiquantitative PCR. We compared the PCR ratio obtained by the current real-time PCR method with that obtained by the previous semiquantitative method [9] in 94 corresponding tumors. The PCR ratio ranged from 0 to 1.38 (*trkA*/β_2-microglobulin) by the previous method, whereas by real-time PCR, the range of the PCR ratio was as wide as 3.26×10^{-4} to 1.98×10^{2} (*trkA*/GAPDH). We also found that the ability of real-time PCR to detect very low levels of *trkA* was superior. The sensitivity of expression analysis may be critical in stratifying patients according to risk, and therefore real-time PCR may be optimal for such expression analyses.

In the current study, high *trkA* expression was linked with better prognosis of the patients. Tumors of patients in younger

ages express significantly higher levels of *trkA*. *MYCN* nonamplified tumors, INSS stage 1, 2, and 4S, favorable histology, and nondiploid tumors also correlated to high expression of *trkA*. In univariate analysis of clinically detected neuroblastomas, previously known prognostic factors, such as *MYCN* amplification, INSS staging, patient's age, DNA ploidy, Shimada histopathology categories, and *trkA* expression, showed significant impact on the survival of patients. These results agree with most of the previous reports that studied *trkA* expression in neuroblastomas [4-11]. The most striking finding in our study was that among age, *MYCN* status, and *trkA* expression, *trkA* expression was solely identified as an independent prognostic factor in the in the clinically detected patient group.

In the current study, we identified the expression level of the previously known *trkA* I and *trkA* II splice variants, but not the recently identified isoform *trkA* III, which has been reported to regulate oncogenic signals in normal cells as well as neuroblastomas [13]. Thus, this study has analyzed the putatively "purely antioncogenic" counterparts of *trkA*. We reviewed the primer sequences of the recent articles that quantitatively analyzed *trkA* expression by competitive PCR or real-time PCR in neuroblastomas and found that most of these studies have designed primer sets to detect all splice variants of *trkA*, including the oncogenic *trkA* III [10,11,19]. Therefore, the true prognostic value of *trkA* may be underestimated in these studies because aggressive neuroblastomas with high *trkA* III expression might also be interpreted as *trkA* expressing tumors.

The recent report by Shimada and colleagues [11] evaluated the prognostic value of *trkA* in neuroblastomas in a relatively large cohort. The study consists of *trkA* expression analysis by competitive PCR in 265 neuroblastoma samples. The authors conclude that *trkA* expression differs significantly between the alive and dead patient groups but does not add significant information to prognostic grouping, as defined by the combination of clinical stage, histopathology, and *MYCN* status. However, there are some factors that need consideration in the interpretation of their results. First, as mentioned above, the primer sets are designed to detect all splice variants of *trkA*, including *trkA* III. Second, the method used in the study is competitive PCR, which has been proved to be quantitative, but yet requires post-PCR manipulations that may affect the measurement of the copy number. Third, the *trk* copy number is not normalized by a reference gene. Regardless of the method used, normalization is widely accepted to be essential to allow accurate comparisons of the results between different samples and conditions [20]. Normalization with internal reference gene is used to control for technical and biological variations introduced during both sample preparation and detection by reverse transcriptase-PCR [21]. It is possible that by refining these effects, *trkA* might gain more statistical power even in large cohort studies.

Our current analysis also needs refinement. The cutoff of high and low *trkA*/GAPDH ratio is defined by the median value of the cohort in this analysis. It is warranted to identify a universal expression marker that provides an optimal cutoff value to stratify the patients' prognosis.

In conclusion, reevaluation of *trkA* expression by innovated sensitive and accurate PCR methods may provide further information on the prognostic value of *trkA*. Our data suggests that *trkA* may have more impact on prognosis of the patients than previously reported by studying the expression of *trkA* I and II, but not *trkA* III. A fine analysis with a large cohort is needed to validate our findings.

Acknowledgments

We thank Dr Yasunori Satoh (Chiba University Clinical Research Center) for reviewing the statistical analysis process.

References

[1] Bolande RP. The neurocristopathies: a unifying concept of disease arising in neural crest maldevelopment. Hum Pathol 1974;5: 409-29.

[2] Brodeur GM, Nakagawara A. Molecular basis of clinical heterogeneity in neuroblastoma. Am J Pediatr Hematol Oncol 1992;14:111-6.

[3] Nakagawara A, Brodeur GM. Role of neurotrophins and their receptors in human neuroblastomas: a primary culture study. Eur J Cancer 1997;33:2050-3.

[4] Nakagawara A, Arima-Nakagawara M, Scavarda NJ, et al. Association between high levels of expression of the TRK gene and favorable outcome in human neuroblastoma. N Engl J Med 1993;328: 847-54.

[5] Borrello MG, Bongarzone I, Pierotti MA, et al. *trk* and *ret* protooncogene expression in human neuroblastoma specimens: high frequency of trk expression in non-advanced stages. Int J Cancer 1993;54:540-5.

[6] Kogner P, Barbany G, Dominici C, et al. Coexpression of messenger RNA for TRK protooncogene and low affinity nerve growth factor receptor in neuroblastoma with favorable prognosis. Cancer Res 1993;53:2044-50.

[7] Miyake M, Suzuki T, Shimada H, et al. High affinity nerve growth factor receptor expression (gp140 *trkA*), N-myc amplification, histopathology, and survival in neuroblastoma. Progr Clin Biol Res 1994;385:163-8.

[8] Kramer K, Cheung NK, Gerald WL, et al. Correlation of *MYCN* amplification, Trk-A and CD44 expression with clinical stage in 250 patients with neuroblastoma. Eur J Cancer 1997;33:2098-100.

[9] Matsunaga T, Shirasawa H, Enomoto H, et al. Neuronal *src* and *trk* A protooncogene expression in neuroblastomas and patient prognosis. Int J Cancer 1998;79:226-31.

[10] Tajiri T, Higashi M, Souzaki R, et al. Classification of neuroblastomas based on an analysis of the expression of genes related to prognosis. J Pediatr Surg 2007;42:2046-9.

[11] Shimada H, Nakagawa A, Peters J, et al. TrkA expression in peripheral neuroblastic tumors: prognostic significance and biological relevance. Cancer 2004;101:1873-81.

[12] Hishiki T, Nimura Y, Isogai E, et al. Glial cell line–derived neurotrophic factor/neurturin-induced differentiation and its enhancement by retinoic acid in primary human neuroblastomas expressing c-Ret, GFRalpha-1, and GFRalpha-2. Cancer Res 1998;58:2158-65.

[13] Tacconelli A, Farina AR, Cappabianca L, et al. TrkA alternative splicing: a regulated tumor-promoting switch in human neuroblastoma. Cancer Cell 2004;6:347-60.

[14] Brodeur GM, Seeger RC, Barrett A, et al. International criteria for diagnosis, staging, and response to treatment in patients with neuroblastoma. J Clin Oncol 1988;6:1874-81.

[15] Sawada T, Hirayama M, Nakata T, et al. Mass screening for neuroblastoma in infants in Japan. Interim report of a mass screening group. Lancet 1984;2:271-3.

[16] Kaneko M, Tsuchida Y, Uchino J, et al. Treatment results of advanced neuroblastoma with the first Japanese study group protocol. Study Group of Japan for Treatment of Advanced Neuroblastoma. J Pediatr Hematol Oncol 1999;21:190-7.

[17] Iehara T, Hosoi H, Akazawa K, et al. *MYCN* gene amplification is a powerful prognostic factor even in infantile neuroblastoma detected by mass screening. Br J Cancer 2006;94:1510-5.

[18] Gotoh T, Hosoi H, Iehara T, et al. Prediction of *MYCN* amplification in neuroblastoma using serum DNA and real-time quantitative polymerase chain reaction. J Clin Oncol 2005;23:5205-10.

[19] Ootsuka S, Asami S, Sasaki T, et al. Analyses of novel prognostic factors in neuroblastoma patients. Biol Pharm Bull 2007;30: 2294-9.

[20] Huggett J, Dheda K, Bustin S, et al. Real-time RT-PCR normalisation; strategies and considerations. Genes Immun 2005;6:279-84.

[21] Thellin O, Zorzi W, Lakaye B, et al. Housekeeping genes as internal standards: use and limits. J Biotechnol 1999;75:291-5.

厚生労働科学研究費補助金
がん臨床研究事業

神経芽腫における標準治療の確立と新規治療の開発に関する研究

平成22年度　総括・分担研究報告書

研究代表者　池田　均

印刷：㈱松井ピ･テ･オ･印刷